Egyptian Geophysical Society
EGS Journal, Vol. 15, No. 1, 19-37 (2017)

STRUCTURAL IMPACT OF THE TERTIARY BASALT SETTING ON THE GROUNDWATER AQUIFERS USING GEOPHYSICAL TECHNIQUES IN THE AREA WEST CAIRO-ALEX. DESERT HIGHWAY BETWEEN THE KM 42 AND 52

M.A. Khaled, A.M. Youssef , M.S. Barseem

Desert Research Center, 1. Matahaf El Matariya street, El Matariya, Cairo, Egypt.

التأثير التركيبى لوضعية بازلت العصر الثلاثى على خزانات المياه الجوفية باستخدام التقنيات الجيوفيزيائية فى المنطقة غرب طريق القاهرة-اسكندرية الصحراوى بين الكيلو ٤٢ و ٥٢

الخلاصـــة: نتائج تفسير ٦٢ جسة كهربية عمودية و بيانات سجلات الآبار المتاحة بمنطقة الدراسة بينت أن التتابع الجيوكهربى يتكـــون مـــن أربـــع وحدات (A B, C and D) طبقا لرواسب البلستوسين و تكوين المغره التابع لعصر الميوسين السفلى و رواسب الأوليجوسين و الحجـــر الجيـــرى لعصر الأيوسين على الترتيب.تم التعرف على ثلاث تكاوين حاملة للمياه الجوفية بمنطقة الدراسة وهى تكوين المغره التابع لعصر الميوســـين الســـفلى (الطبقات الجيوكهربية B2&B3) ، خزان الاوليجوسين (الطبقات الجيوكهربية C4,C5 and C6) و الحجر الجيري لعصر الايوسين (الوحـــدة D) الذى يتميز بامكانات مائية ضعيفة بالمقارنة بتكوين المغرة وخزان الاوليجوسين نتيجة لضعف التشققات. فرشات البازلـــت لحقبـــة الثلاثـــى (الطبقـــة الجيوكهربية C1) تعمل كطبقة مميزة تفصل خزان المغرة الذى يعلوها عن خزان الأوليجوسين الذى يوجد اسفلها. هذه الفرشات البازلتيه توجد علـــى عمق ضحل (٤متر) فى الجزء الجنوب الشرقى من منطقة الدراسة بينما يزيد العمق تدريجيا فى اتجاه الشمال الغربى لأكثر من ٢٢٠ متر.هذه الزيادة فى العمق نتيجة لتأثير مجموعة من الفوالق الطبيعية السلمية ذات رميه فى اتجاه الغرب و الشمال الغربى. هذه الفوالق أدت الى ميل فرشات البازلت لحقبة الثلاثى و صخور الأوليجوسين التى توجد اسفلها فى اتجاه الغرب و الشمال الغربى. هذه الفوالق رفعت خزان المغرة فى الجزء الجنوب الشرقى مـــن منطقة الدراسة و فى نفس الوقت عملت على ذيادة سمك نفس الخزان لأكثر من ٢٥٠ متر حيث لم يتم الوصول للسطح السفلى لهذا الخزان فى الجزء الشمال الغربى من منطقة الدراسة. حركة الرفع فى الجزء الجنوب الشرقى من منطقة الدراسة ادت الى وجود الطبقة الحاملة للمياه لعصر الايوســـين مقابلة لخزان الأوليجوسين . الفوالق التركيبية أدت الى اتصال هيدروليكى بين خزانى المغرة و الأوليجوسين على جانبى الفوالق . هذا الاتصال يقلـــل من جودة مياه خزان المغرة و فى نفس الوقت يحسن من جودة خزان الأوليجوسين نتيجة لخلط مياه الخزانين.

وجد أن النسبة المئوية لحجم الطين الصفائحى المتداخل مع الرمال لخزانى المغرة و الأوليجوسين لها عامة علاقة طردية مع الملوحة. خزان المغـــرة يتميز بالقيم الأقل بينما خزان الأوليجوسين يتميز بالقيم الأعلى. الآبار التى تنتج من الخزانين معا تتميز بقيم متوسطة لحجم الطين الصفائحى وعلى هذا الأساس فان المحتوى الطينى له تأثير مباشر على جودة المياه الجوفية طبقا لذلك فان الجزء الشمال الغربى من منطقة الدراسة له الأولوية لحفر أبـــار جديدة .

ABSTRACT: *The interpretation results of 62 Vertical Electrical Soundings (VES) and the available well logging data in the study area revealed that the geoelectrical succession is consisting of four units (A, B, C and D) corresponds to Pleistocene deposits, Lower Miocene Moghra Formation, Oligocene deposits and Eocene limestone respectively. Three water-bearing formations were identified in the study area. These water-bearing formations are namely, the Lower Miocene Moghra aquifer (geoelectrical layers B2 and B3), the Oligocene aquifer (geoelectrical layers C4, C5 &C6) and the Eocene limestone (unit D). The Tertiary basaltic sheet (geoelectrical layer C1) acting as a marker bed separating the overlying Moghra aquifer from the underlying Oligocene aquifer. The Tertiary basalt acts as a marker bed separating the overlying Moghra aquifer from the underlying Oligocene aquifer. The Tertiary basalt is found at shallow depths (4m.) in the southeastern part of the study area whereas; the depth increases gradually northwest wards to more than 220 m. This is mainly attributed to the effect of a group of normal step faults with downthrown side west and northwest wards. These faults cause the convergence of Moghra and Oligocene aquifers along the two sides of the faults making a hydraulically connection of the two aquifers*

The estimated shale volume percentage from natural gamma-ray logs with the sand of Lower Miocene Moghra and Oligocene aquifers revealed that the Moghra aquifer has the lowest values but the Oligocene aquifer has the highest values. According to these results, the northwestern part of study area has the priority of drilling new wells.

Key words: *Structure, Tertiary Basalt, Groundwater, Aquifers, Vertical Electrical, Sounding (VES).*

INTRODUCTION

Reclamation of the desert areas lying to the west of the Nile Delta has continued since many decades and received special governmental attention. Therefore, there is a sever need for groundwater to use in irrigation and other development objectives. Due to the complex geologic structures and the setting of the basaltic sheets

from one side and the random drilling activities for groundwater from the other side, many farm owners faced serious problems of water depletion and salinities which have negative effects on the agricultural investments on such area and consequently, huge losses of money. The occurrence of groundwater is mainly controlled by the geologic setting, basaltic sheet configuration, lateral and vertical lithologic variations, tectonic and structural frameworks, and the sedimentological and mineralogical properties of the subsurface rocks. So, it is necessary to define these all factors and their impacts on the groundwater occurrences. The geoelectrical studies are the cheapest and the most suitable techniques to give important information on the subsurface geology including the configuration of aquifers and the structures affecting them (e.g. El Badrawy and Soliman 2003; Al Temamy and Barseem 2010 and Sultan et al, 2011).

The Tertiary basaltic sheet is a marker rock unit separating the overlying Lower Miocene aquifer (Moghra) and the underlying Oligocene aquifer. Therefore, detecting the basaltic sheet and the accompanied subsurface geologic structure as well as its impact on the groundwater occurrence are the main objectives of this study.

The present work is an attempt to apply the geoelectrical resistivity sounding and the well logging data of the available drilled wells in the area of study to delineate the following:

- The sedimentary succession and its vertical and lateral facies changes.
- The water bearing formations and their distributions.
- The distribution of the basaltic sheet and the associated subsurface structures and their impact on the groundwater occurrence.

The area of study is a part of the south west of the Nile Delta (Fig.1). It is bounded by latitudes 30° 3' and 30° 8' 30" N and longitudes 30° 49' to 30° 56' 15" E covering an area of about 75 Km^2 and extends along Cairo-Alexanderia Desert Highway. It is bounded northeast words by the Cairo-Alexandria Desert Highway, Garet El Hadadein ridge from the east, Gebel Hamza from northwest and Ras El Hohod from the South.

Geomorphology, geology and hydrogeologic settings:

Geomorphologically, the West Nile Delta area, lies within the arid province of Egypt. The climate of this region is characterized by long hot summer and short mild rainy winter. The geomorphologic units prevailing in the west of the Nile Delta comprise alluvial plains, structural plains, southern tablelands and drifting sands (Shata and El Fayoumy1967, Sanad 1973 and Attia 1975). The area of study lies in the structural plains geomorphic unit. This plain lies to the south of old alluvial plain. It is extensive pavement plain that consists of a number of alternating ridges and depressions reflecting the lithologic units and geologic structures. A number of alternating ridges and depressions around the study area can be also recognized. These ridges are Garet El Hadadien plateau (233 m) and Gebel Hamza (110 m), where the depressions are represented by Wadi El Farigh (-4 m) and Wadi El Natrun (-23 m). Generally, the southern part of this area is covered by Aeolian sand and gravels with occasional clay interbeds of Holocene and Pleistocene deposits (Said, 1962 and Abdel Baki, 1983). The ground elevation of area of study ranges from 159 m at the south east to 110 m at northwest. The general gradient is towards the north western direction.

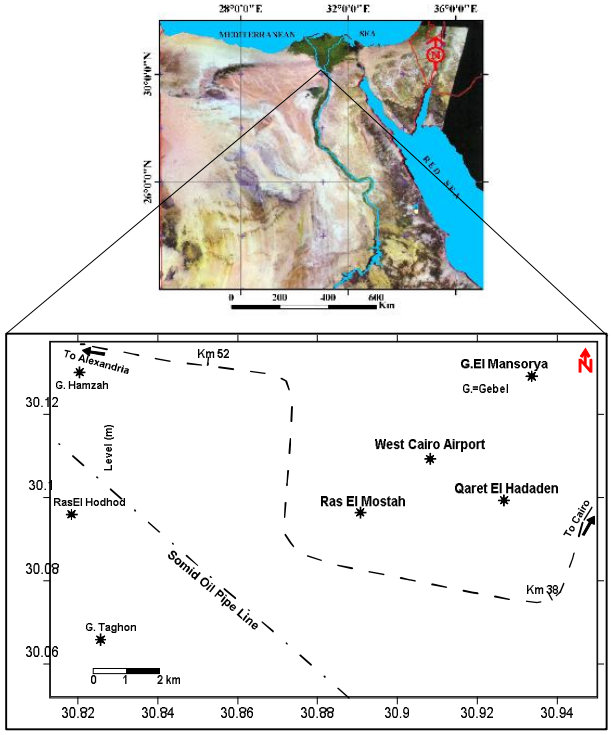

Fig. 1: Location map of the study area.

Geologically, The west of the Nile Delta is covered by sediments and sedimentary rocks ranging in age from Late Cretaceous to Quaternary (Shata, 1961) and (Shata and El-Fayoumy, 1967). The study area as a part of the West of the Nile Delta comprised rock units varying from Oligocene to Quaternary (Fig 2). The stratigraphic succession from the base to the top is described as follows:

1- The Tertiary deposits are related to four periods. Eocene, Oligocene, Miocene and Pliocene. They are represented by limestone, dolomite, marls, claystone, sandstone and conglomerate. The lithology of Eocene is represented by chalky, clayey and sandy limestones grading into marls and clays as well as sandy marls and clays (El-Shazly et al, 1975).The Eocene deposits crop out on the surface at the vicinity of Abu Roash uplift, Said, (1962) and Shata et al. (1962). The Oligocene

deposits are represented by Sand, ferriginous sandstone, sand clay, clayey sand and clay .The Oligocene deposits are exposed near Abu Roash domal structure to the southeast of the investigated area. It is unconformably underlain by Upper Cretaceous rocks (Said, 1962; Shata et al, 1962; and El Shazly et al, 1975). Oligocene deposits are overlain by dissected basaltic sheets of Abu Zaabal Formation. Through the drilled water wells by the Desert Research center (DRC 1992 -2013) and private companies along Cairo-Alex. Desert Highway, the basaltic sheets are detected in some localities at depth ranging from few meters up to 220 m. with a thickness varying from 8-32 m. The detection of the basaltic sheets at different levels reflects the effect of the structures on the geologic succession and the groundwater occurrence, flow and quality in consequence.

The Miocene deposits cover wide parts of the area. These deposits are represented by El Moghra Formation which is mainly exposed on Wadi El Farigh area and its extension. According to Said (1962), El Moghra Formation is mainly composed of coarse sands, sandstone and clay interbeds with vertebrate remains, silicified woods and gravels at base.

The Pliocene includes two major lithostratigraphic units. The lower unit is assigned to the Lower Pliocene and is represented by dark clay facies having thickness exceeding 200m underneath the Nile Delta (Sanad, 1973). The upper unit belongs to the Middle and Upper Pliocene is almost exposed at Wadi El-Natrun depression and consists of sandstone alternated with shally limestone and limestone (Omara and Sanad, 1975).

2- The Quaternary deposits cover a large portion of the area under consideration and its adjacent areas. These deposits are composed of unconsolidated clastic deposits. It is not easy to differentiate between the Pleistocene and Recent deposits. The idealized stratigraphic section of the study area is shown in table 1 (according to the previous discussion).

Geologic structure:

The main regional structures affecting the study area and its vicinities have been discussed by many authors, Said (1962), Shata et al. (1962), and Abd El-Rahman (1996). The tectonic setting of the west Nile delta is represented by folding and faulting.

(A) Folds: Two fold systems had affected the west Nile Delta area. According to their orientation, these fold systems are the Syrian arc system (NE-SW) as Abu Raoash anticline and the Clysmic system (NW-SE) as Wadi El Farigh and Wadi El Natroun anticline (Said, 1962), (Shata et al., 1962) and (Omara and Sanad, 1975).

(B) Faults: The detected faults are mainly arranged parallel to the surface folds. They belong to the Syrian arc system (NE-SW) and the Clysmic system (NW-SE), with low vertical displacements (El Ghazawi and Attwa, 1994). According to Abd El-Rahman (1996) the southwestern portion of the Nile Delta had been subjected to intensive movements which resulted in dissecting the area with 17 normal faults striking in NE-SW and NW-SE directions. Some faults are major ones and define the regional structural pattern and other minor faults, however, had been initiated as direct effect of the major ones and form some local structural pattern such as horsts and grabens. These faults should have a direct impact on the groundwater occurrence as well as flow direction and gradient.

Hydrogeologically, the water-bearing formations in the west Nile Delta are represented by Pleistocene, Pliocene, Lower Miocene, Oligocene and Eocene aquifers. The groundwater aquifers in the western Nile Delta are connected hydraulically (Sharaky et al, 2007). The last three aquifers are represented in the study area and can be summarized as the followings:

- Lower Miocene aquifer is represented by the Moghara Formation which covers the western part of the study area. This aquifer composed of sand, gravels, sandstone and clay interbeds with vertebrate remains and silicified wood (Said, 1962). This aquifer is present under semicofined condition. It is overlain by Quaternary deposits and underlain by the Oligocene basaltic sheet. The groundwater salinity is almost fresh and this reflect the direct recharge from the great basin underlain Rosetta branch through fault plains (Ahmed, 2002).
- Oligocene aquifer is composed of sand, sandy clay, clayey sand, sandy gravels, clay and sandstone interbeds with thin limestone band. The Oligocene aquifer is found to exist under confined to semiconfined conditions. The confined conditions prevail in the localities where the basaltic sheet and the underlying clay beds extent over a wide subsurface area. The semiconfined conditions are due mainly to the sandy clay and clay interbeds within the aquifer. The Oligocene aquifer is more clayey and/ or higher in salinity or both than the Miocene aquifer (Abdel Rahman, 1996). The environmental isotopes indicate that the main recharging sources for the Oligocene are paleo water (El Abd, 2005).
- Eocene aquifer, Lithologically, it is represented by chalky, clayey and sandy limestone grading into marls and clays as well as sandy marls and clays. In the subsurface, it is composed of clays and shales with limestone at the base (El Shazly et al., 1975). According to Said (1962), these rocks are composed of brownish limestone and shaly sand beds. This aquifer is of limited water potentiality due to its contents of limestone and clay.

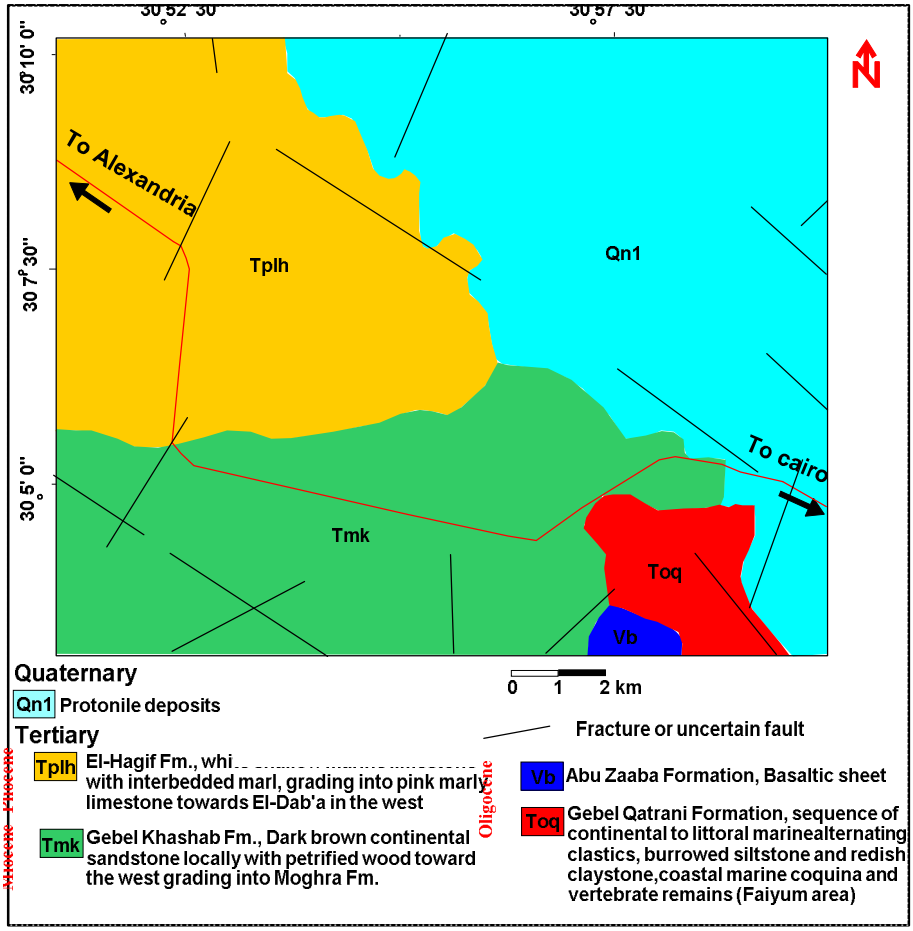

Fig. 2: Geologic map of the area of study (After CONOCO, 1987).

Table (1): The identified stratigraphic units in the study area and its environs.

Age		Rock Unit	Lithologic description
Quaternary	**Holocene**	Aealian deposits	Quartz
	Pleistocene	Alluvial deposits	Sand, clay, silt and high gray gravel
Tertiary	**Pliocene**	Upper unit Lower unit	sandstone with shaly limestone and limestone dark clay facies
	Miocene	Moghra Formation	Coarse sands, sandstone, clay interbed with Vertebrate remains, silicified woods and gravels.
	Oligocene	Abu Zaabal Formation	Basalt
		Abu Roash Sandstone Formation	Sand, ferriginous sandstone, sand clay, clayey sand, clay and sandy gravels.
	Eocene	Maadi Formation	Chalky, clayey and sandy limestone, clay, shale and marls with limestone at base.

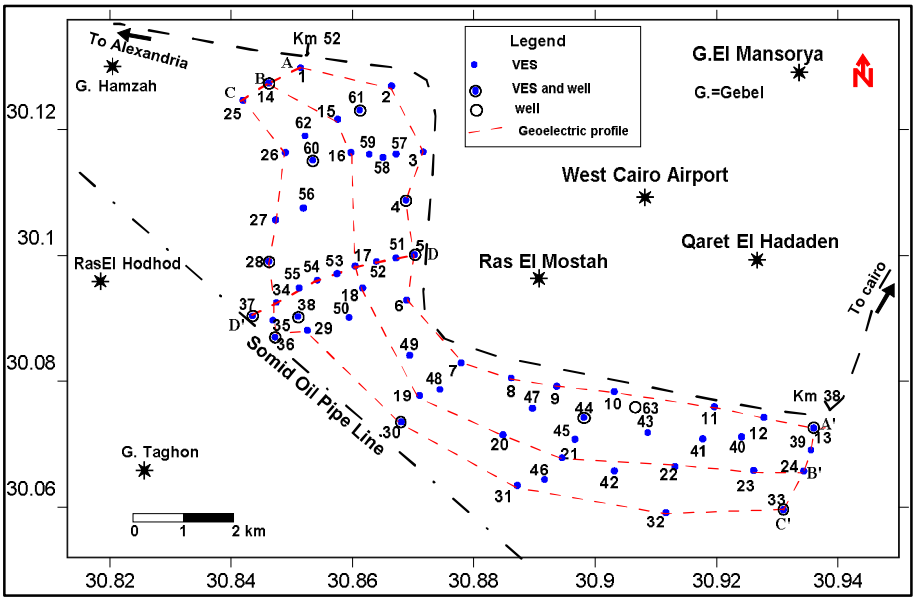

Fig. 3: Location of VES stations, wells and geoelectrical profiles.

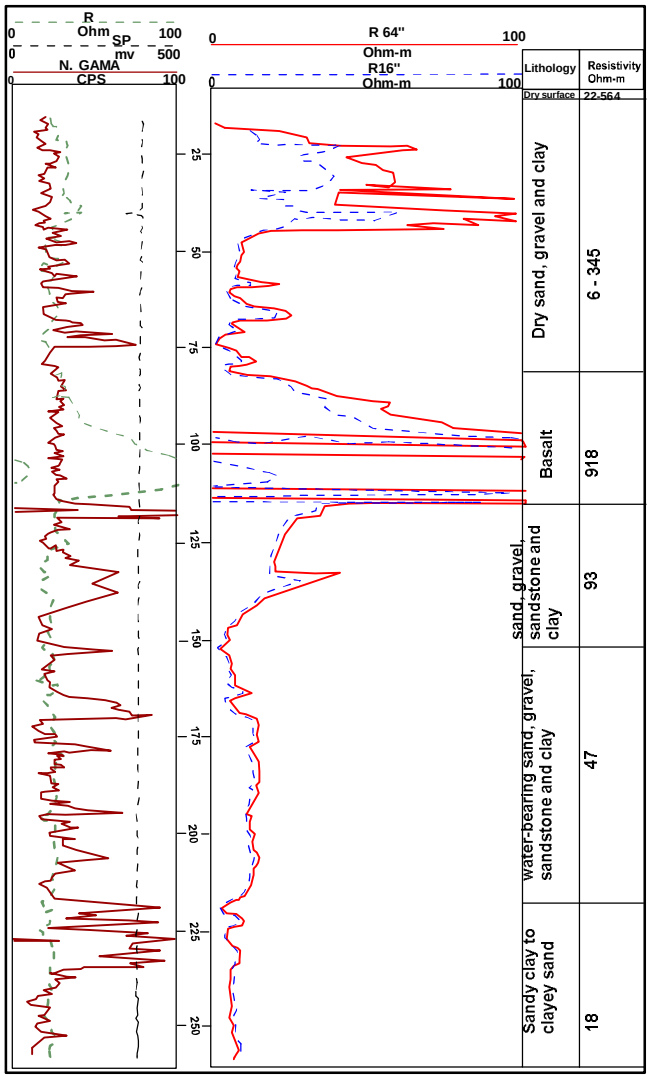

Fig. 4: Electrical and lithological logging data of the drilled well beside VES no. 44 as well as the interpretation results of resistivity sounding.

Methodology:

To fulfill the objective of the present study, a geoelectrical survey was carried out through the conducting of 62 vertical electrical soundings (Fig.3). The geoelectrical measurements were carried out using the direct current resistivity meter "Terrameter", models SAS 300 C and SAS 1000. The instruments automatically calculate the ratio ΔV/I (R) with high accuracy. The well known Schlumberger configuration of electrode separation (AB/2) ranging from1 up to 2000 m was applied. Some VES was carried out beside drilled wells to use its data in the correlation and calibration of the VES model parameters (layers' resistivities and thicknesses) of the interpreted geoelectrical data with the geologic information (lithology and thickness). An example of the well logging data is shown in fig. 4.

The available electric logs of the drilled wells in the investigated area are used to adjust the limits of different layers, determine the depth to basaltic sheet, locate the depth to water and finally, eight logs of these wells are used to calculate the shale volume of the Lower Miocene Moghra and Oligocene aquifers and their contribution on the groundwater quality. The shale volume (shv) was estimated from natural gamma-ray logs using the following formula (Steiber, 1973 and Bhuyan and Passy, 1994).

V_{sh}= 0.5IGR/1.5-IGR …… (Steiber, 1973)

$I_{GR} = GR_{log} – GR_{min}/ GR_{max}- GR_{min}$ .....(Bhuyan and Passy, 1994)

where, V_{sh} is the shale volume

I_{GR} is the gamma-ray index GR_{log} is the gamma-ray for zone log reading

GR_{min} is the gamma-ray value of clean formation (shale –free)

GR_{max} is the gamma-ray reading of typical shale

The topographic map scale (1:50,000) and the Global Positioning System (GPS) were used to determine the accurate locations and ground elevations of the sites of both the geoelectrical soundings and drilled wells.

The quantitative interpretation technique was applied to determine the thicknesses and true resistivities of each VES station using the measured field curves. The resistivity interpretation was carried out using both of the computer programs Resist (1988) and IPI2win (2003) to compute the true depths and resistivities for each VES curve.

Interpretation techniques:

The field data of the VESes have been interpreted qualitatively and quantitatively to delineate the subsurface sequence of the geoelectrical layers in the area of study.

Concerning the qualitative interpretation: According to the obtained VES curves, the resistivity value along the first and second cycles (AB/2 = 1 to 100) represent surface and near surface variations. They reflect heterogeneity characterizing the surface layers. This heterogeneity is due to the clay beds intercalating the sand and gravel deposits. In going downwards on the field curves, (third cycle at AB/2 > 100m.) show different types which reflects heterogeneity of lithology due to structure effects. The dominant field curves in the study area are; HKH, KHQ, HKQ, HAK, HKQA and KHQ types (Fig. 5), which indicate the heterogeneity of lithologic composition as well as the structure effects.

The Quantitative interpretation Provides the true resistivities, depths and thicknesses of the geoelectrical layers. These parameters become the main source of information which can delineate the subsurface geologic succession, structures and water-bearing formation, then presented in the form of cross sections and different types of maps. The VES curves were interpreted quantitatively by constructing a model for each curve, using the computer programs RESIST, (Van Der Velpen 1988) and IP2win (2003). It is a non automatic iteration method in which the measured field data are compared with data calculated from an assumed model. The models were prepared with the aid of the collected data of some wells near the VES stations. An example of the interpretation results of VES no. 36 beside a well is given in figure 6. In order to reach an optimum correlation between the geoelectrical layers and the geologic units, some successive geoelectrical layers have been grouped together in one layer. The interpretation results of the VESes were used to construct six geoelectrical cross sections A-A`, B-B`, C-C', A-C, D-D' and A'-C' (Fig. .3).

RESULTS AND DISCUSSION

The results of the quantitative interpretation of the 62 VES curves as well as the constructed geoelectrical cross sections A-A`, B-B`, C-C', A-C, D-D' and A'-C' (Fig. 3) revealed that the subsurface of the area is vertically distinguished into 4 main geoelectrical units (A, B, C and D). These units illustrate the geoelectrical sequences, lateral and vertical variation of the different layers, depth to water bearing layers, depth and thickness of basaltic sheet and the accompanied subsurface structures. The description of this geoelectrical succession is given here after.

The first geoelectrical unit **"A"** represents the dry surface zone which extends from the surface downwards to a depth varying from 1.5 m at VES 13 to 4 m at VES No. 29 and has a resistivity ranging from 9 Ohm-m at VES No. 30 to 4989 Ohm-m at VES No. 23. The wide range of resistivity may be due to the change in lithology from gravels, sand to clay. This unit is closely correlated to the Pleistocene and Pliocene deposits.

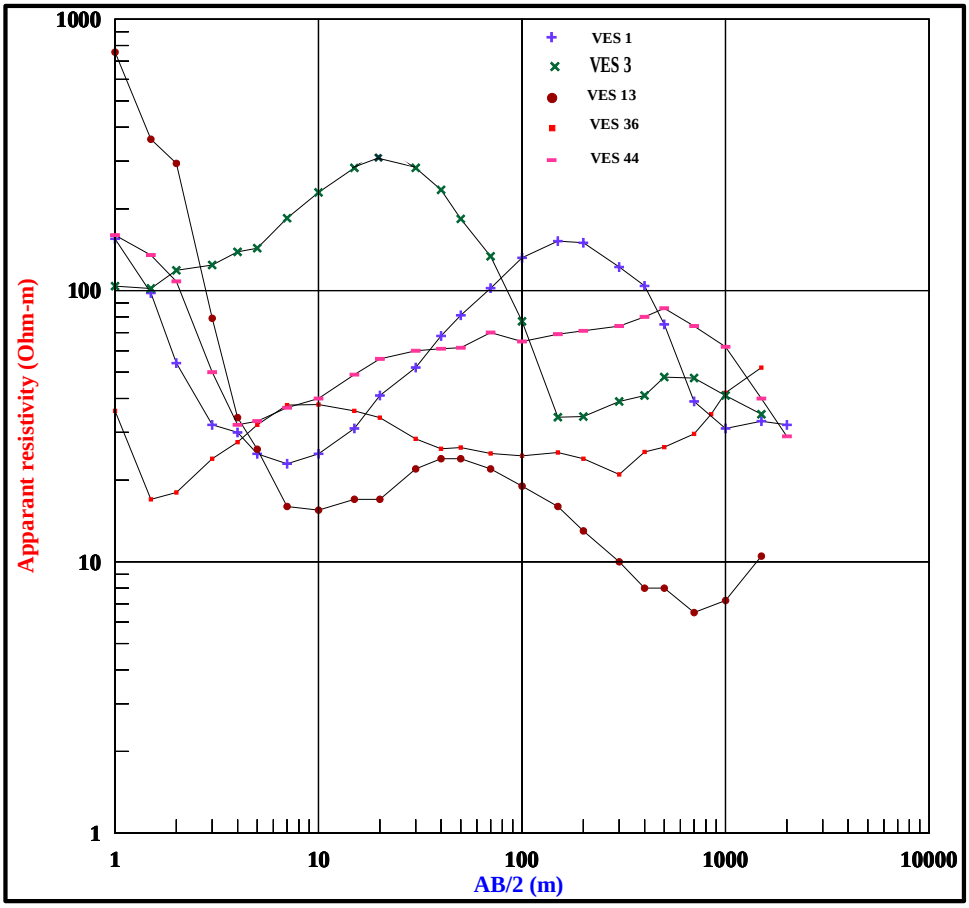

Fig. 5: Example of the field curves in the study area.

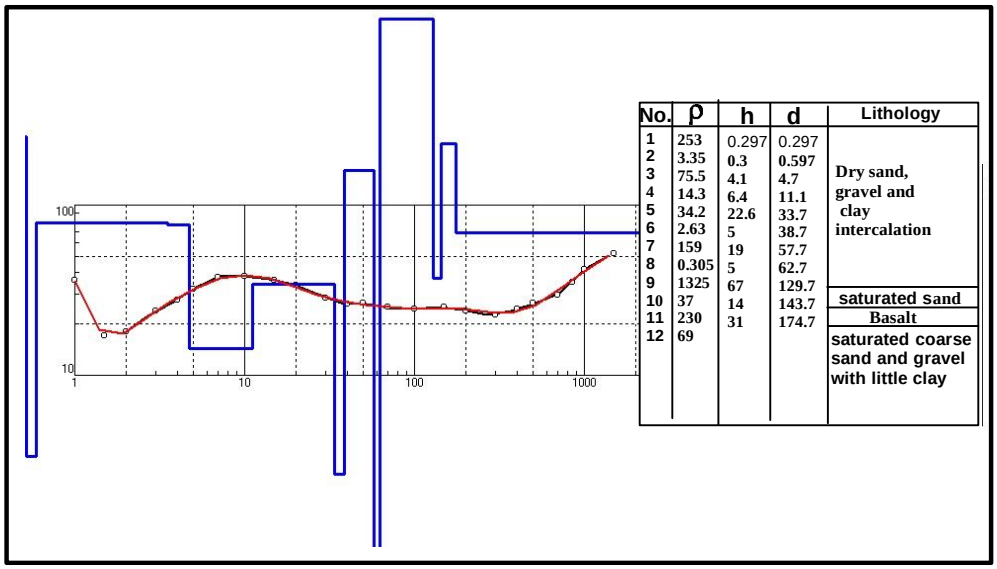

Fig. 6: Interpretation results of VES no. 36 beside well (IP2win program).

The second geoelectrical unit **"B"** consists of three geoelectrical layers (B1, B2 and B3). This unit is equivalent to Lower Miocene Moghra Formation. The first geoelectrical layer **"B1"** has a wide range of resistivity values. It ranges from 5 Ohm-m at VES 11 to 488 Ohm-m at VES 4 (Table 2). It has a thickness ranging from 2.5 m. at VES 12 to 158 m. at VES 5. These resistivity values correspond to multi-beds of dry sand, gravel sandstone and clay. Sometimes, clay bed lies at the bottom of this layer. The second geoelectrical layer **"B2"** has resistivity values ranging from 36 ohm-m at the middle part (VES 7) to 66 Ohm-m at the northwestern part (VES 15) of study area (Fig. 7). This resistivity value corresponds to sand water-bearing. The thickness of this layer ranges from 13m at VES 6 to 72 m at VES 27. The bottom of this layer is unreached at some locations. The third geoelectrical layer **"B3"** has resistivity value varying from 14 Ohm–m (VES 25) to 34 Ohm-m. (VES26). This layer was detected in the northwestern part and its lower bottom unreached.

The Third geoelectrical unit **"C"** consists of six geoelectrical layers (C1, C2, C3, C4 , C5 & C6). This unit is equivalent to Oligocene deposits. The first geoelectrical layer **"C1"**is equivalent to the basaltic sheet. It has a wide range of resistivity values corresponds to the position of these sheets. The basaltic sheet lies in the dry zone has resistivity values more than 360 Ohm-m whereas that lies between the water-bearing formations has resistivity values less than 262 Ohm-m. This is due to the presence of wet fractures in basalt. This agrees with the results of Abd El Rahman (1996), Mabrouk (1998), Ezz El Deen (1999) and concerned with the basaltic sheets of the southwest of the Nile Delta. The thickness of these sheets varies from 8 m at VES 13 to 32 m. at VES 29 in the area of study. The second geoelectrical layer **"C2"** has resistivity values ranging from 9 Ohm-m at VES 22 to 187 Ohm-m at VES. 20. This resistivity value corresponds to dry sand, gravel, sandstone and clay. The thickness of this layer ranges from12 m at VES 13 to 77 m. at VES 32. The third geoelectrical layer **"C3"** has resistivity value varying from 14 Ohm.m at VES 20 to 33 Ohm.m at VES 23. This layer corresponds to dry sandy clay to clayey sand. It has a thickness varying from 124m at VES 33 to 131m at VES 13. The fourth geoelectrical layer **"C4"** has resistivity values increase from 35 Ohm.m in the middle part (VES 34) to 76 Ohm.m in the northwestern and southeastern parts (VES11) of the study area (Fig. 8). This layer corresponds to water-bearing sand, gravel, sandstone, sometimes interbeds of limestone and clay. The thickness of this layer varies from30 m at VES 11 to 75 m at VES 22. The fifth geoelectrical layer **"C5"** has resistivity value varying from 14 Ohm.m at VES 20 to 25 Ohm.m at VES 22. This layer corresponds to sandy clay to clayey sand. The lower limit of this layer was not reached. The sixth geoelectrical layer "C6" was detected only at the southeastern part of study area. It has resistivity value varying from 5 Ohm.m at VES 24 to 16 Ohm.m at VES 13. This layer corresponds to clay to saturated sandy clay. It has a thickness varying from 24m at VES 33 to 37m at VES 24.

The last detected unit is unit "D". It was detected at the southeastern part only. Its resistivity value ranges from129 Ohm-m at VES 33 to 161 Ohm-m at VES 12. These resistivity values correspond to Eocene limestone of low potential groundwater. The bottom of this unit was not reached with the used current electrode separation.

Geoelectrical cross sections:

To avoid the repetition, the main observation and conclusions from the six constructed geoelectrical cross sections A-A`, B-B`, C-C', A-C, D-D' and A'-C' (Figs. 9, 10, 11, 12, 13 and 14) are listed in the following:-

1- The three geoelectrical cross sections (A-A`, B-B` and C-C') illustrate the whole succession of the four identified geoelectrical units (A, B, C and D). On the other hand, the other three geoelectrical cross sections (A-C, D-D' and A'-C') illustrate only some of the detected succession.

2- Generally, the basaltic sheets are found at shallow depths in the southeastern part (4m) and increase, gradually northwest wards to 222.5 m. near the northwestern part. On the other hand, a greater depth than 222.5m is expected at the extreme northwestern part. This gradation in depths is due to the action of a group of step normal faults with downthrown side to the northwest.

3- Geoelectrical unit "B" has a maximum thickness at the extreme northwestern part where its base was not detected. Its thickness decreases towards the middle part of the study area and uplifted in the southeastern part due to the structures effects.

4- The layers of geoelectrical unit "C" generally, deeply plunged northwestwards. Therefore, it is expected to be detected at greater depths in the northwestern part due to the structure effect.

5- The resistivity value of the water-bearing layers in both of units "B" and "C" decreases with depth (resistivity of layer B2 > B3 and resistivity of layer C4 > C5>C6) due to the increase of salinity and/ or increase of clay content or both.

6- Some dry layers that lie above the water table become water-bearing when lying below the water table. This concept is related to the layers C2 and C4 that have the same composition, where C2 lies above the water table (in the dry zone) and C4 lies below the water table. Also, the layers C3 and C5 have the same composition. The layer "C3" east the fault "F1" lies in the dry zone whereas layer C5 west the fault "F1" is water-bearing.

7- Geoelectrical layers C3, C6 and Unit D (Eocene limestone) were detected only at the extreme southeastern part of the study area.

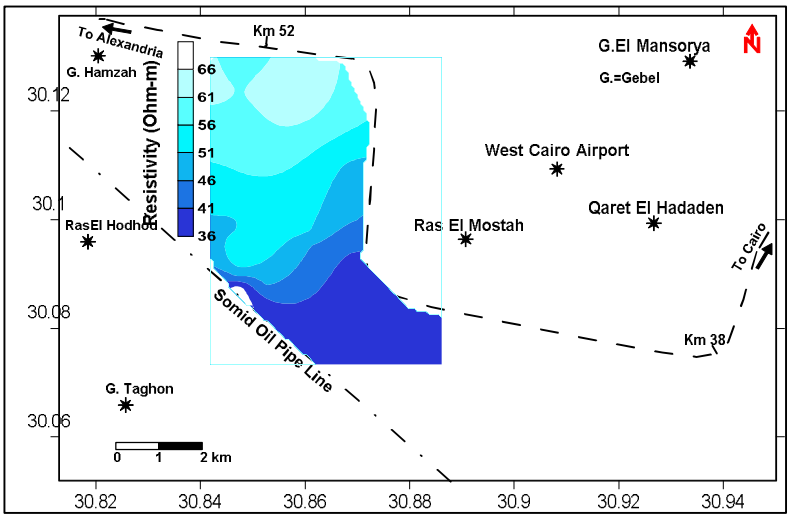

Fig. 7: Resistivity value of the water-bearing layer (B2)

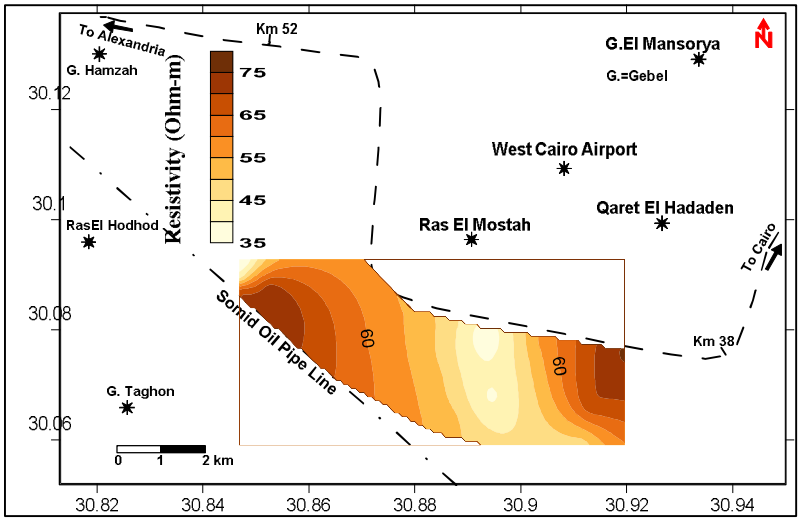

Fig. 8: Resistivity value of the water-bearing layer (C4)

Table (2): Resistivities and thicknesses ranges.

Geoelectrical units	Geoelectrical layers	Resistivity (Ohm-m)	Thickness (m)
A		9 (VES30) - 4989 (VES 23)	1.5 (VES 13) - 4 (VES 29)
B	B1	5 (VES 11) - 488 (VES 4)	2.5 (VES 12) - 158 (VES 5)
	B2	36 (VES 7) - 66 (VES 15)	13 (VES 6) -72 (VES 27)
	B3	14 (VES25) - 34 (VES 26)	----------
C	C1	242 (VES5) -1001 (VES 11)	8 (VES 13)-32 (VES 29)
	C2	79 (VES 22) -187 (VES 20)	12 (VES 13)-77 (VES32)
	C3	14 (VES 20) - 33 (VES 23)	124 (VES 33)-131 (VES 13)
	C4	35 (VES34) -76 (VES 11)	30 (VES 11)-75 (VES 22)
	C5	14 (VES 20) -25(VES22)	----------
	C6	5 (VES 24) -16 (VES13	24 (VES 33-37 (VES24)
D		129 (VES33) -161 (VES 12)	----------

8- The groundwater potential is high in both quantity and quality in the northwestern part than that in the southeastern part. This high potential is due to the larger thickness of the water-bearing layers (Moghra aquifer) that consist of sand and clayey sand. On the other hand, the water-bearing layers in the southeastern part have more clay content (Oligocene and Eocene deposits) and consist of sand, clayey sand, sandy clay, clay and limestone.

Hydrogeologic setting:

The water-bearing formations in the study area were classified according to the geological, hydrogeological and the drilled wells information as well as the geophysical results into three main aquifers. The first aquifer is the Lower Miocene aquifer (Moghra Formation). It is composed of sand, gravels sandstone and clay interbeds. These sediments are overlain by the dry part of Moghara sediments and Quaternary deposits and underlain by the Oligocene basaltic sheet (Abu Zaabal Formation). This aquifer is considered to exist under semiconfined conditions. Two connected water-bearing layers (geoelectrical layers B2 and B3) were detected. The first layer has a thickness generally, increases from 13 m at the middle part of study area to 73m at the northwestern part (Fig.15).

The second water-bearing layer "B3" was detected only at the extreme northwestern part. It has generally, a lower resistivity value than the layer B2 due to the increase of the clay content downward. It varies from 14 Ohm.m to 35 Ohm.m corresponds to sandy clay to fine sand. The Lower bottom of this layer was not reached with the applied current electrode separation.

The second aquifer is the Oligocene aquifer which underlies the basaltic sheet and consists of sand, clayey sand, sandy clay, limestone inter-beds and clay. It is found to exist under confined to semiconfined conditions. Two connected water-bearing (geoelectrical layers C4 and C5) were detected. The first layer (C4) lies beneath the basaltic sheet (layer C1) if the basaltic sheet overlain by Moghra aquifer (geoelectrical layer B2) or below the dry layer C3 (sand, gravel, sandstone and clay). This layer has a thickness generally, increases from 30 m. in the southeastern part of study area to 75m with a general increase westwards (Fig. 16). The increment in thickness northwestwards for both layer B2 and C4 is coincide with the downthrown side direction of the normal step faults affecting the study area. The second water–bearing layer **"C5"** has resistivity value varying from 14 Ohm-m to 25 Ohm–m. This layer corresponds to sandy clay to clayey sand. The bottom of this layer was not detected at the most of the sounding stations.

The constructed geoelectrical cross-sections (Figs. 9 to 14) revealed that, the two aquifers of Moghra and Oligocene are hydraulically connected as a result of the normal step faults affected the study area. So, the depth to water bearing layers (B2 and C4) in the study area varies from 130 m in the northwestern part of the study area to 160.5 m. in the southeastern part (Fig.17). On the other hand, the level to the upper surface of the water-bearing layers (B2 and C4) varies from -18 m below the sea level at the northwestern part to -6 m below the sea level at the southeastern part of the study area (Fig, 18). Therefore, the expected direction of flow for the groundwater may from the southeast to northwest and from east to west directions (Fig.18). Geoelectrical layer “C6” makes as aquifer at some VES stations at the extreme southeastern part. It has a low groundwater potential due to its high clay content. Its resistivity value varies from 5 Ohm.m to 16 Ohm.m. This layer corresponds to clay to saturated sandy clay. Its thickness varies from 24m to 37m. The last detected aquifer was detected only at the extreme south eastern part of the study area. It is equivalent to Eocene limestone (unit D). This aquifer has low potential comparable with the Moghra and Oligocene aquifers due to the decrease in its fracture size (secondary porosity). Its resistivity value varies from from129 Ohm-m at VES 33 to 161 Ohm-m.

To shed light about the quality of groundwater of both Moghra and Oligocene aquifers, this can be illustrated through the calculated shale volume (Shv) of the Lower Miocene Moghra and Oligocene aquifers from natural gamma-ray logs (table 3). The calculated shale volume (Shv) revealed that, the shale volume content has a direct relation with the salinity. The Moghra aquifer has the lowest shale volume and salinity and the Oligocene aquifer has the highest shale volume and salinity. On the other hand, the wells taping both Moghra aquifer and Oligocene aquifer has intermediate shale volume and salinity. Although the well no. 36 has the lowest shale volume percentage but has intermediate salinity (1500 ppm) due to the intrusion of limestone interbeds with high ratio in geoelectrical layer C4. Therefore, it can be concluded that the clay content and limestone interbeds raise the salinity of Oligocene aquifer (layers C4 and C5). On the other hand, the low clay content of Moghra aquifer (layer B2 and B3) reflected in the low salinity of this aquifer.

Impact of the associated structures of the Tertiary basalt on the groundwater occurrence:

The geologic setting of Tertiary basalt (geoelectrical layer C1) is mostly used to differentiate between the overlying Moghra aquifer (geoelectrical layer B2) and the underlying Oligocene aquifer (geoelectrical layer C4). It has a wide range of resistivity values corresponding to, the position of these sheets. The basaltic sheets lie in the dry zone has resistivity values more than 350 Ohm-m whereas, that lies between the water-bearing formations has resistivity values less than 262 Ohm-m. (Fig.19). The basaltic sheets have a thickness generally, increases from 8m at the extreme southeastern part to 32 m at the northwestern part (Fig. 20). The depth to basaltic sheet is found near the earth surface (4m) at the southeastern part whereas; it increases northwestwards to more than 22o m (Fig.21). It is expected, to be found at greater depths at the extreme northwestern part.

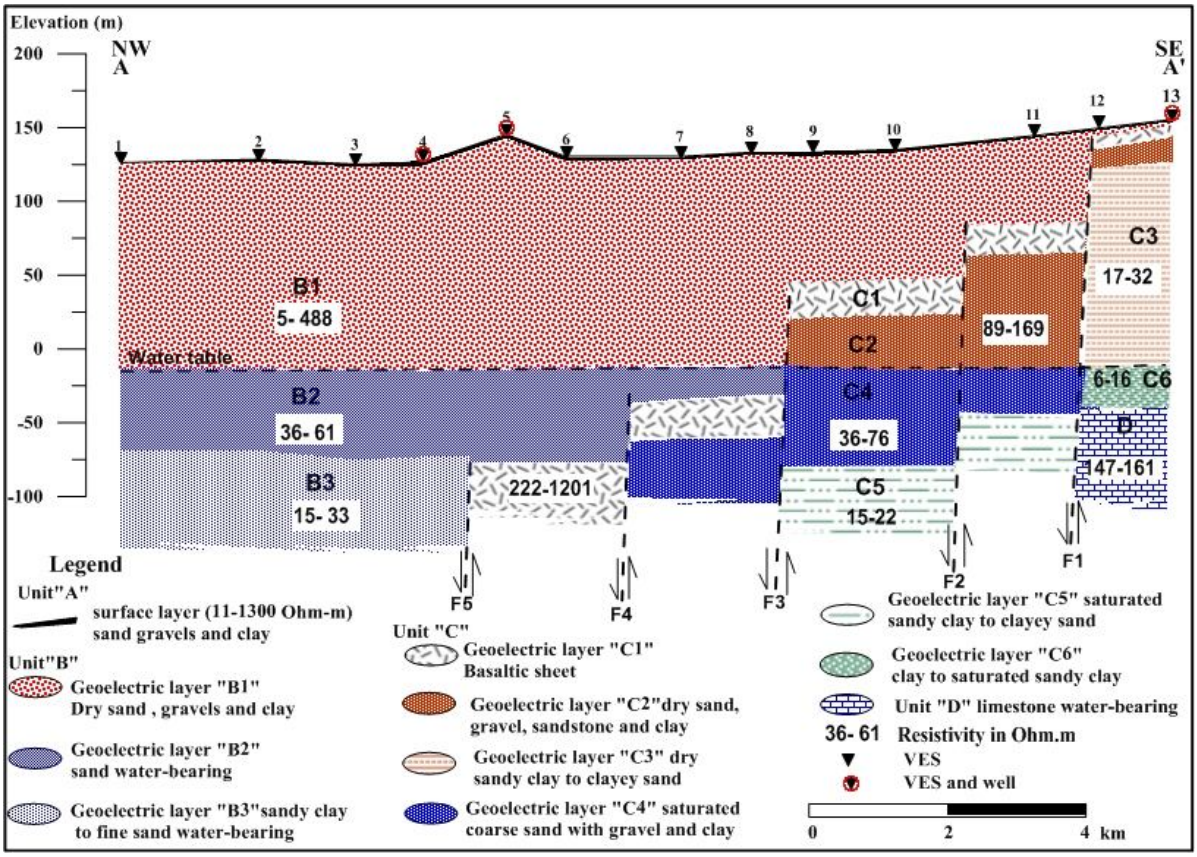

Fig. 9: Geoelectrical cross section A-A'.

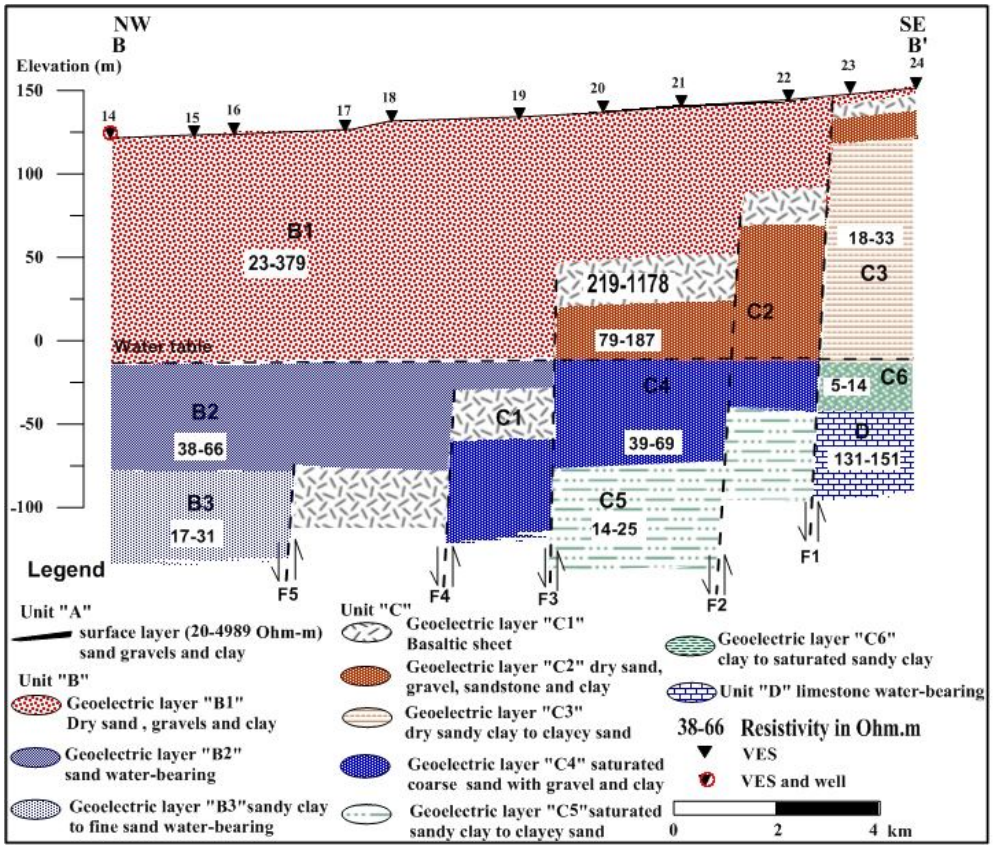

Fig. 10: Geoelectrical cross section B-B'.

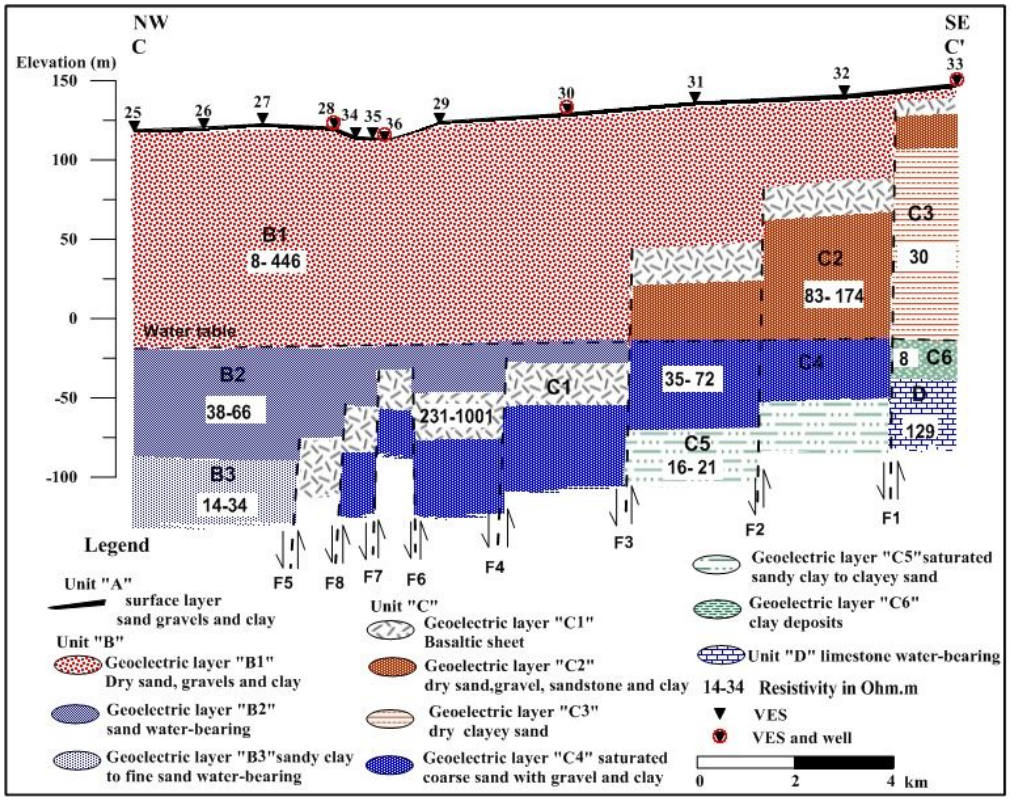

Fig. 11: Geoelectrical cross section C-C'.

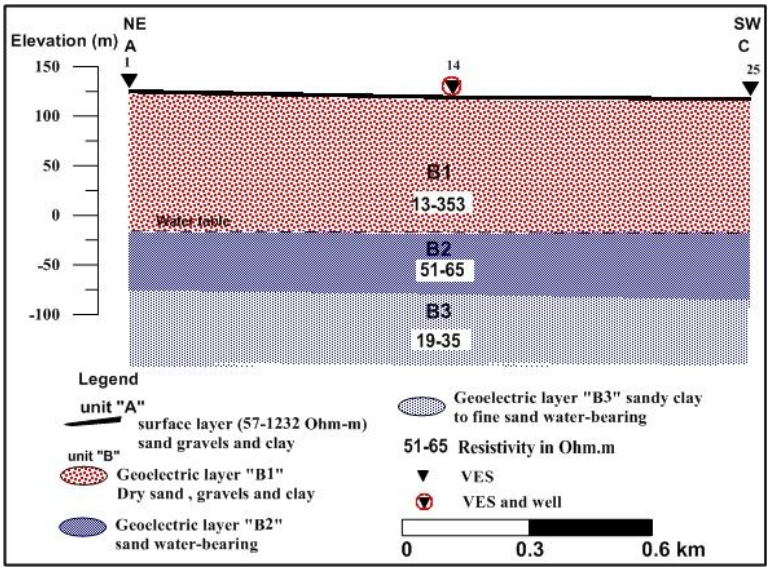

Fig. 12: Geoelectrical cross section A-C.

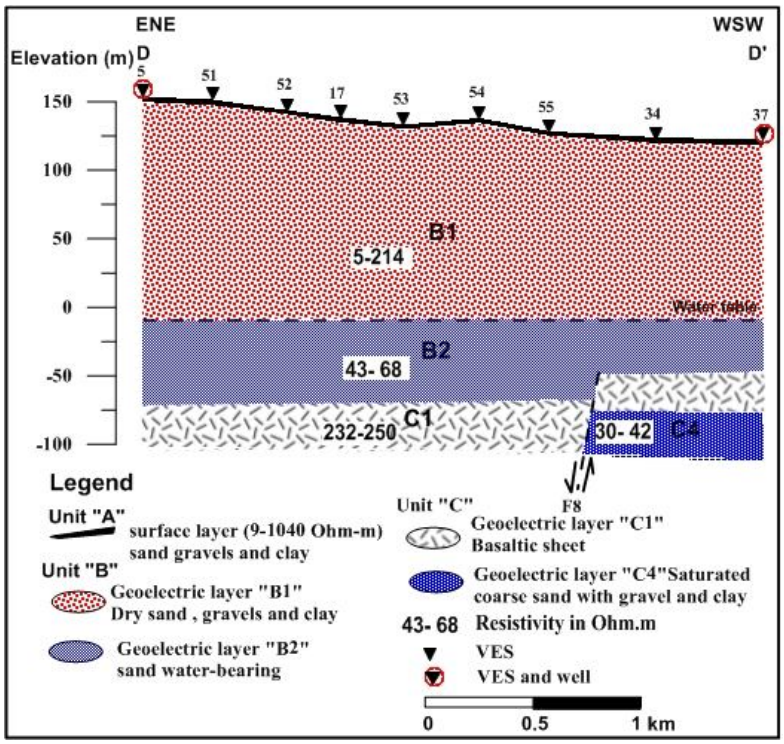

Fig. 13: Geoelectrical cross section D-D'.

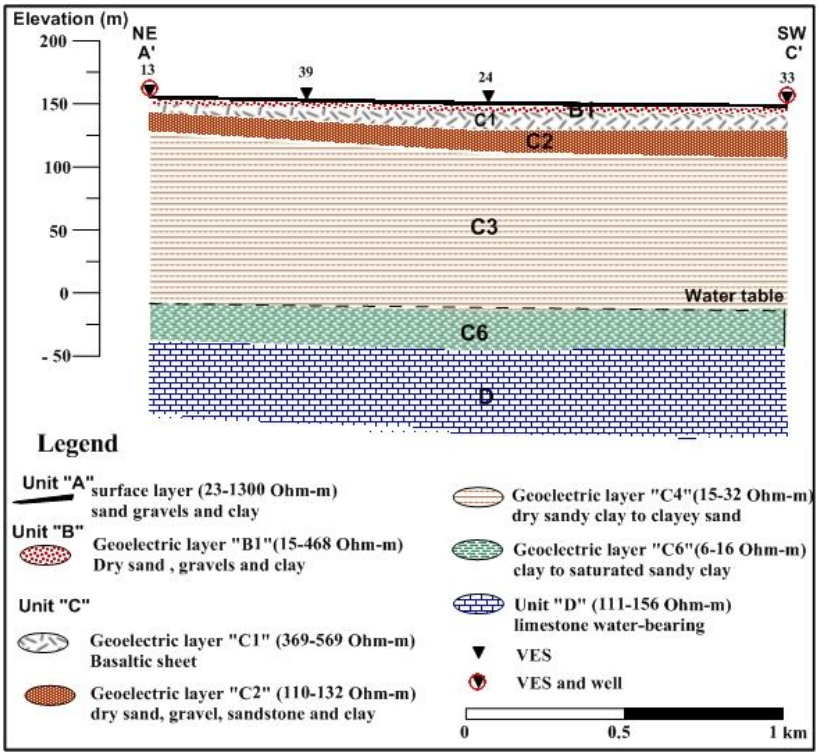

Fig. 14: Geoelectricalal cross section A'-C'.

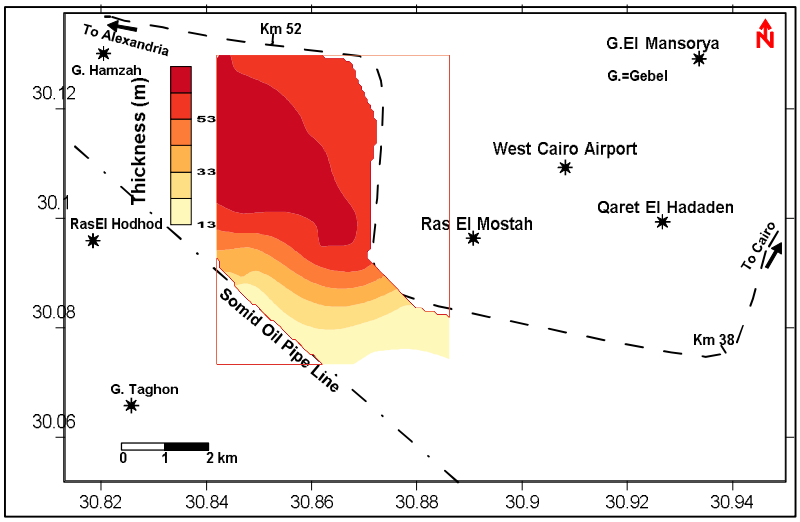

Fig. 15: Isopach map of the water-bearing layer (B2).

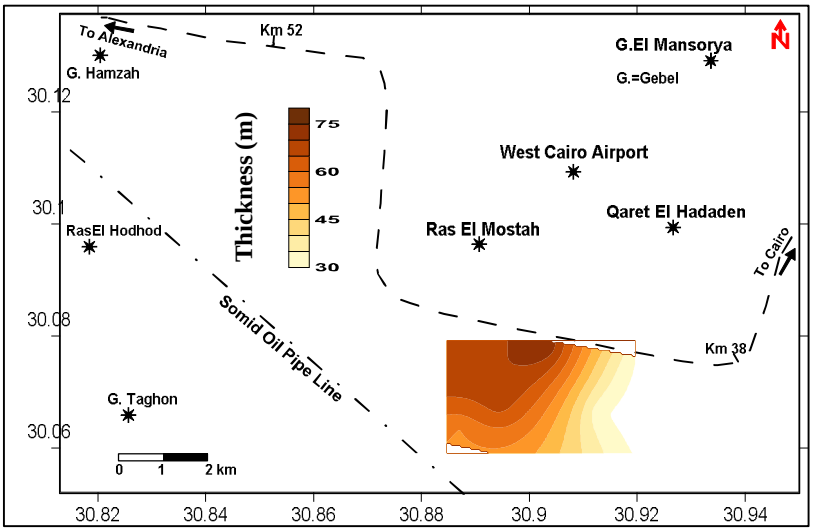

Fig. 16: Isopach map of the water-bearing layer (C4).

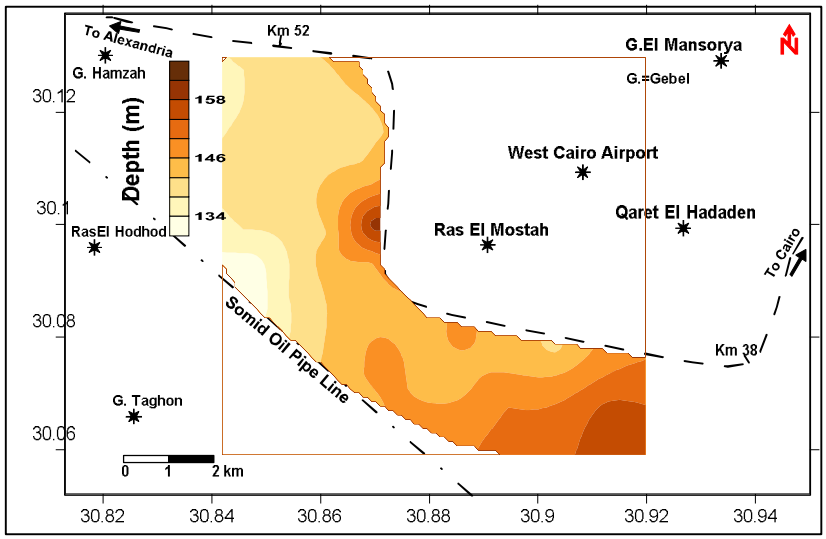

Fig. 17: Depth to water-bearing layers (B2 and C4) in the study area.

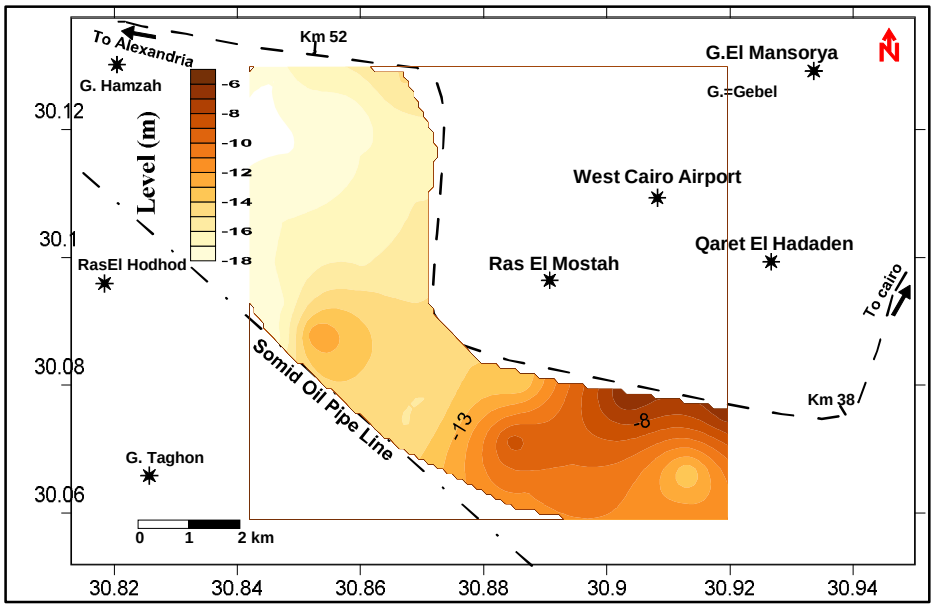

Fig. 18: Level of water-bearing layers (B2 and C4) in the study area.

Table (3): Shale volume (Shv) percentage and salinity.

Well at VES No.	Investigated depth(m)	Shv percentage	Salinity in (ppm)	Water-bearing layer
5	160-225 (layer B2)	16.2	1100	Layer B2 of Moghra aquifer
14	135-205 (layer B2) 205-250 (layer B3)	15.3	950	Layers B2 & B3 of Moghra aquifer
36	129-144(layerB2) 168-186 (layer C3)	12	1500	Layer B2 and layer C4 of Moghra and Oligocene aquifers respectively
38	129-160(layerB2) 183-205 (layer C3)	21	1600	Layer B2 and layer C4 of Moghra and Oligocene aquifers respectively
44	150-217 (layer C3) 217-260(layer C4)	26.3	2100	Layers C4 & C5 of Oligocene aquifer
60	140 -204 (layer B2) 204-220 (layerB3)	12.5	800	Layers B2 and B3 of Moghra aquifer
61	143-203 (layerB2) 203-250 (layerB3)	14.1	915	Layers B2 & B3 of Moghra aquifer
63	153-185 (layer C3) 185- 250 (Layer C4)	22.5	1830	Layers C4 & C5 of Oligocene aquifer

This increment is due to the structural effect. The level of the top of t he basaltic sheet ranges from 158m above the sea level in the southeastern part of the study area to -78 below the sea level in the middle part of study area (Fig. 22). This steep variation in basaltic sheet level is demonstrated well also in the 3-D basalt relief surface which clarifies the variation in the relief of basalt due to the structure effect (Fig. 23). From these maps in addition to the constructed geoelectrical cross-sections (Figs.9-14) and the data of available wells, inferred structural map was deduced (Fig. 24). This map indicates that the area of study is affected by 5 major faults (F1, F2, ….and F5) and 3 minor faults (F6, F7 and F8). These faults have a direct impact on the groundwater occurrence in the study area. The water bearing layers "B2 & B3" were not detected in the extreme southeastern part of the study area where these layers are uplifted. In the same time, the layer "B2" was detected with a small thickness and the layer "B3" was not detected in the middle part of the study area for the same previous causes. In the same manner, the water-bearing layer "C4" was not detected east the fault F1 and instead, the layer "C3" which has the same lithology of layer C4 lies above the water-bearing level due to uplift movement at these locations. This uplift movement causes the presence of layer C6 and Eocene aquifer (Unit D) east the fault F1 to meet the Oligocene water-bearing layer "C4 &C5" west the fault F1. The structure faults "F3 and F4" lead to the hydraulically connection of Moghra aquifer (layer B2) and Oligocene aquifer (layer C4) along the two sides of the faults F3 and F4. As the Moghra aquifer is fresher than the Oligocene aquifer, this hydraulically connection decreases the quality of Moghra aquifer and enhances the quality of Oligocene aquifer due to the mixing between the two aquifers. The depth to the upper surface of both El Moghara water-bearing (layer B2) and the Oligocene water-bearing (layer C4) appears as one surface due to the effect of the normal step faults (F1-F3). The normal step faults F1 to F5 have downthrown side north and northwestwards. These faults cause the Oligocene basalt and the underlying layers go deeper northwestwards. Therefore, the basaltic sheet and the underlying Oligocene aquifer were not detected at the extreme northwestern part and the Moghra aquifer was detected with a larger thickness. The minor faults F6 and F7 form a small horst between them so the Moghra water-bearing layer "B2" was detected with a small thickness. Also the minor fault F8 has a downthrown side northward.

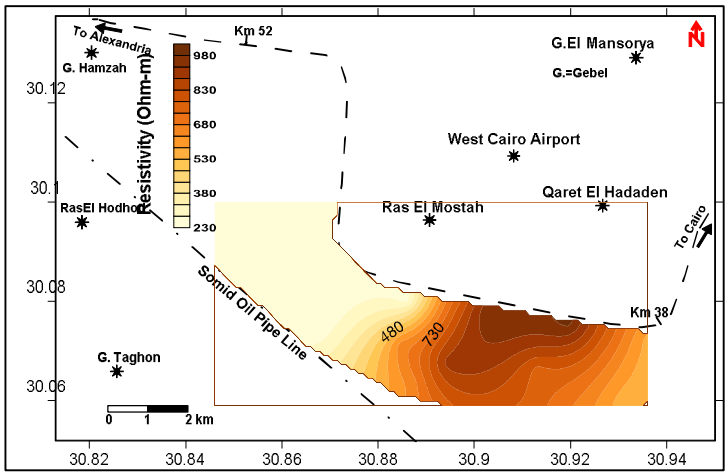

Fig. 19: Resistivity of geoelectrical layer "C1".

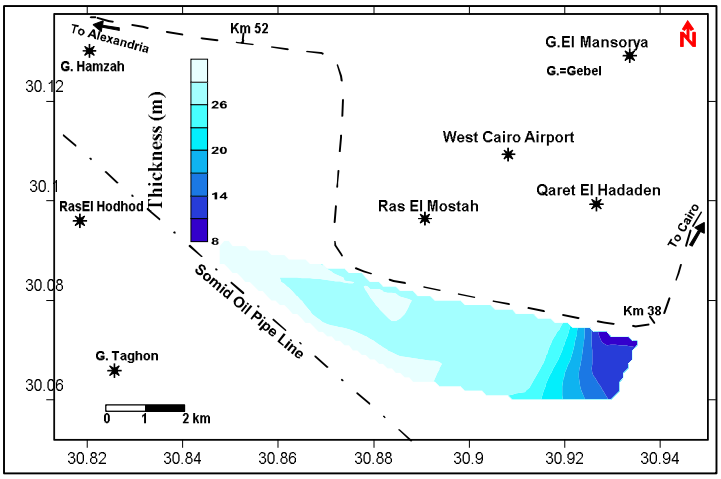

Fig. 20: Isopach map of geoelectrica layer "C1".

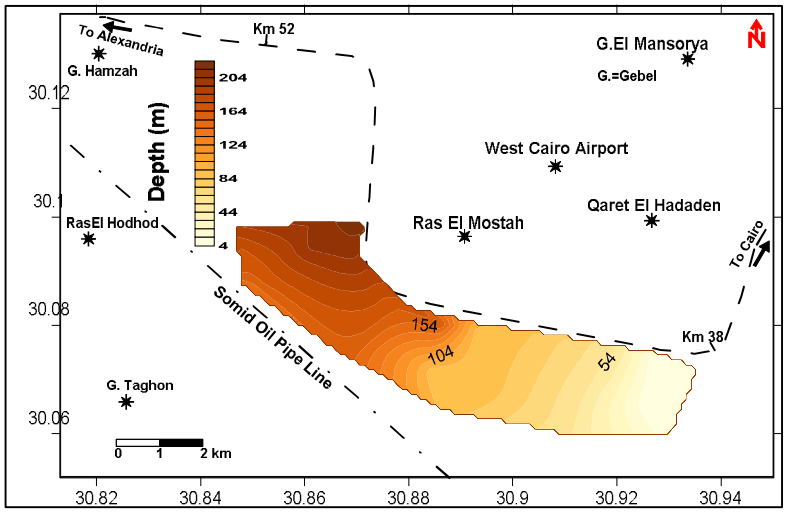

Fig. 21: The depth to the top of geoelectricalalal layer "C1"(basaltic sheet).

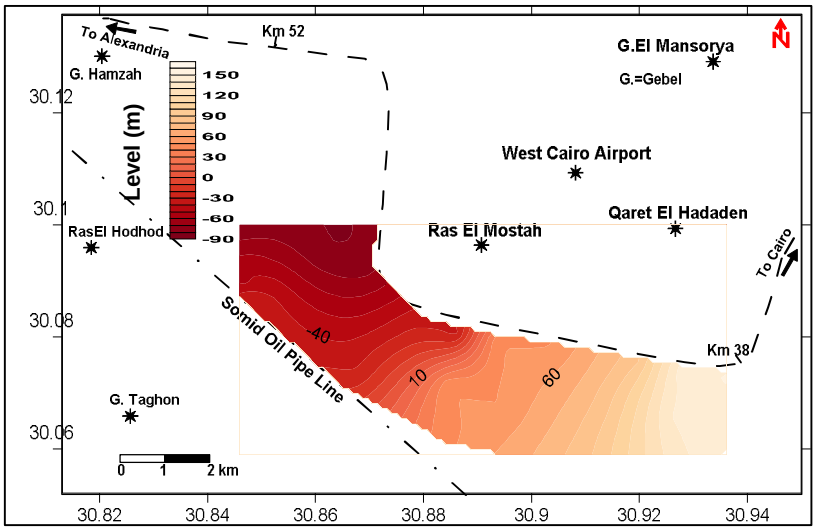

Fig. 22: The level of the top of geoelectricalalal layer "C1"(basaltic sheet).

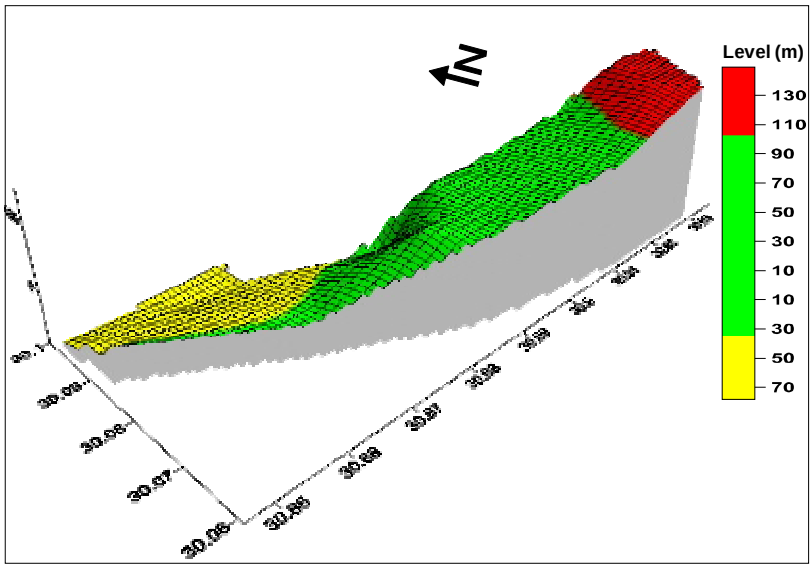

Fig. 23: 3-D basalt relief surface (geoelectricalalal layer C1).

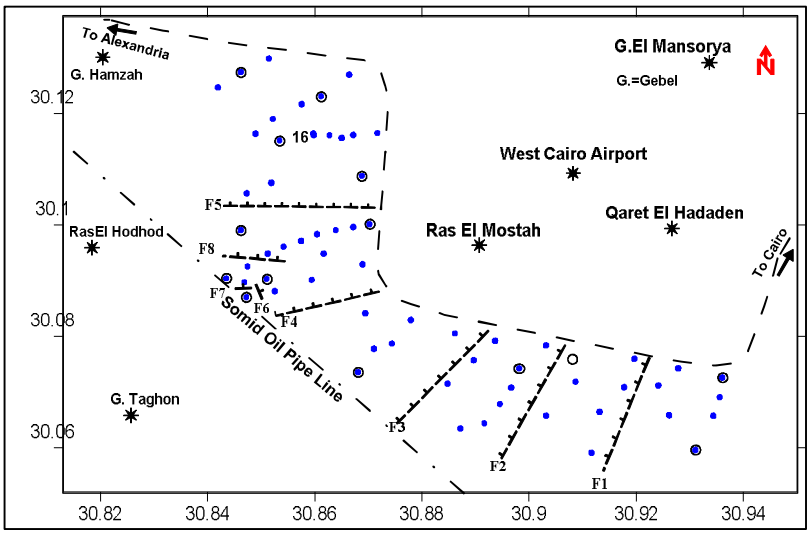

Fig. 24: Inferred structure in the study area.

CONCLUSIONS AND RECOMENDATIONS

It can be concluded that, the inferred Tertiary basaltic sheet from the Vertical Electrical Sounding interpretation results and from the drilled wells data is used to differentiate between the overlying Moghra aquifer and the underlying Oligocene aquifer. The associated structures to the basaltic sheets cause the slope of the basaltic sheet (layer C1) and the underlying Oligocene aquifer (geoelectricalalal layers C4 and C5) northwestwards. These structures uplifted the Moghra aquifer (Geoelectricalalal layers B2 and B3) in the southeastern part. In the same time, the inferred faults lead to the meeting of both Moghra aquifer (geoelectricalalal layer B2) and Oligocene aquifer (geoelectricalalal layer C4) along the two sides of the faults. Therefore, the two aquifers are hydraulically connected. The estimated shale volume from natural Gamma ray logs revealed that the shale volume has a direct relation with the measured salinity. The wells tapping the Moghra aquifer have the least shale volume and salinity but the wells tapping the Oligocene aquifer have the highest shale volume and salinity. On the other hand, the wells tapping both Moghra and Oligocene aquifers have intermediate shale volumes and salinity. As the Moghra aquifer (geoelectrical layer B2 and B3) has the largest thickness southwest wards and has the lowest shale volume and salinity it is recommended to drill new wells in the northwestern part of the study area.

REFERENCES

Abdel Baki, A.M.A., (1983): "Hydrogeological and hydrogeochemical studies in the area west of Rosetta branch and south El-Nasr canal" PH.D. Thesis, Fac. Sci., Ain Shams Univ. 156p.

Abd El Rahman, A.A., (1996): "Geophysial study on the groundwater conditions in the area southwest of the Nile Delta between Abu Raoash and El Khatatba road" M.SC. Thesis, Fac. Sci. Ain Shams Univ. 116p.

Ahmed, K.A., (2002): " Hydrogeological studies on the groundwater aquifers in the northwest Cairo", Ph. D. Thesis, Fac. Sci. Al Azhar Univ. 113P.

Al Temamy, A.M.M. and Barseem, M.S.M. (2010): Structural impact on the groundwater occurrence in the Nubia Sandstone aquifer using geomagnetic and geoelectricalalalal techniques, northwest Bir Tarfawi, East El Oweinat area, Western Desert, Egyptian Geophysical Society (EGS) Journal, Vol. 8, No. 1, pp. 47-63.

Attia, S.H. (1975): Pedology and soil genesis of Quaternary deposits in the region West of the Nile Delta (Northeast of Wadi El Natrun Ph.D. Thesis, Fac. Sci. Ain Shams Univ., 228p.

Bhuyan, K., and Passey, Q.R. (1994): "Clay estimation from Grand Neutron-Density logs" Trans. SPWLA 35 th Annual logging symposium. Paper DDD. 12P.

Continental Oil Company CONOCO (1987): Geologic Map of Egypt 1:500 000 series, Sheet.

Desert Research Center (1991-2013): Geoelectrical studies on some areas of Cairo – Alex. High Way, Egypt. Internal Reports, Publications of the Desert Research Center.

El Abd, E.A., (2005): " The geological impact on the water bearing formations in the area southwest Nile Delta, Egypt" Ph.D. Thesis, Fac. Sci., Menufiya Univ., Egypt, 319 p.

El-Badrawy, H.T. and Soliman, M. R. (2003): Subsurface evaluation of south Kharga Oasis area, south Western Desert, Egypt. Egyptian Geophysical Society (EGS) Journal, vol. 1, No. 1, p. 31-41.

El Ghazawy, E.M. and Attwa, S.M., (1994): "Contribution of some structural elements to the groundwater condition in the southwestern portion

of the Nile Delta" Desert Research Center. Cairo, Egypt. P.

Ezz El-Deen, H.M. (1999): "Implication of the subsurface structures on the groundwater aquifers in the area between Km 38 and Km 46, Cairo-Alexandria Desert Road" pp. Bull. E.G.S. Proc. of the 6th Ann. Meet. P.111-130.

El Shazly, E.M., Abdel Hady, M.A., El Ghawaby, M.A., El Kassas, I.A., Khawasik, S.M., El Shazly, M.M., and Sanad, (1975): "Geologic interpretation of landsat satellite images for West Nile Delta area": Remote Sensing Center, Academy of Scientific Research and Technolog, Cairo, Egypt, p.38

Gomaa, M.A.A. (1995): Comparative hydrogeological and hydrogeochemical study on some aquifers, West of Nile Delta, Egypt. Ph.D thesis, Fac. Sci., Ain Shams Univ., Cairo, Egypt, p.236.

IPI2Win Program (2003): Programs set for 1-D VES data interpretation. Dept. of Geophysics, Geological Faculty, Moscow University, Russia

Mabrouk, M.A. (1998): "Possibilities and limitations of recognizing the Tertiary basalt on the apparent resistivity curves, southwest Nile Delta area, Egypt" Mansoura Sci. Bull (C Nat. Sci. and Phys. Sci.), Vol. 25 (1), P. 25-40.

Omara, S.M. and Sanad, S. (1975): Rock stratigraphy and structural features of the area between Wadi El Natrun and the Moghara Depression, Western Desert, Egypt. Geol. Jb, Bl. 6, Hannover,: p.46-73.

Said, R. (1962): "The geology of Egypt" Elsvier Publishing Co., Amsterdam, New Yourk, 377p.

Sanad, S. (1973): Geology of the area between Wadi El Natrun and the Maghra Depression. Ph.D. Thesis. Fac.Sci. , Assiut Univ. , Assuit, Egypt, 184 p.

Sharaky, A.M., Atta, S.A.; El Hassanein, A.S. and Khallaf, K.M.A. (2007): "Hydrochemistry of groundwater in the western Nile Delta aquifers, Egypt" 2nd International Conference on the Geology of Tethys, , Cairo University

Shata, A.A. (1961): "The geology of groundwater supplies in some arable lands in the desert of Egypt. Internal report, Desert Institute, Cairo, Egypt.

Shata, A.A., Pavlov, M., and Sanad, K.F., (1962): "Preliminary report on the geology, hydrogeology and groundwater hydrology of Wadi Ell ?Natrun and adjacent areas": Internal report desert Institute, Cairo, Egypt, p. 159.

Shata, A.A., and El fayoumy, I.F., (1967): "Geomorphological and morphopedological aspects of the West of the Nile Delta with special reference of Wadi Natroun". Desert d'Egypt; T.XVIII., No.1, p.1-28.

Steiber, R.G., (1973): "Optimization of shale volumes in open hole logs.", Jour. Pet. Tech

Sultan. A.S., Fernando, A.M. and Helaly, A.S. (2011): "Integrated geophysical interpretation for the area located at the eastern part of Ismailia Canal, Greater Cairo, Egypt. Arab Jour. Geosci. P 735-753.

Vander Velpen, B.P.A. (1988): Computer program "Resist", Version 1.0.t, a package for the processing of the resistivity sounding data, M.Sc. Research project, Delf. Netherlands.